*Journal of Marine Research, 44,* 713–738, 1986

# Rossby adjustment over a step

by A. E. Gill[1], M. K. Davey[1], E. R. Johnson[2] and P. F. Linden[3]

ABSTRACT

The adjustment of a rotating fluid to a geostrophic equilibrium is now a classical problem in the theory of rotating fluids and is associated with the name of Rossby because of his pioneering work in this subject. The case of particular interest here is the one where the fluid is initially at rest but has a discontinuity in surface elevation along a certain line. If the bottom is flat, the adjustment gives rise to a jet flowing along the line of the initial discontinuity, the width of the jet being the Rossby radius of deformation. This paper examines how the flow is modified when the bottom is not flat, but has a step-like discontinuity running perpendicular to the line of the initial jump in surface elevation, giving rise to double Kelvin waves which propagate along the step. Flow is thus diverted parallel to the step, and behind the wave front there is no mass flux across the step.

The effect of adding a vertical coast perpendicular to the step is also considered. When the double Kelvin wave propagates offshore, it leaves behind a state with no transport across the step. With propagation toward the coast, however, there is pinching of the longshore current into a narrow boundary layer.

The problem is examined using (a) linear analysis, (b) laboratory experiments, and (c) numerical experiments.

## 1. Introduction

In 1937 and 1938, Rossby considered the mechanisms by which pressure and velocity distributions in the atmosphere and ocean undergo mutual adjustment toward a geostrophic equilibrium in which pressure gradients are balanced by the Coriolis acceleration. He illustrated the process by considering a flat bottomed shallow layer of fluid with an initial nonequilibrium distribution of surface elevation and velocity. A classical case is the one where the initial velocity $(u, v)$ is zero but the surface elevation $\eta$ has a discontinuity along a certain line $x = 0$, i.e.,

$$u = v = 0, \eta = \eta_0 \operatorname{sgn} x \quad \text{at } t = 0 \tag{1.1}$$

1. Hooke Institute for Atmospheric Research, Clarendon Laboratory, Parks Road, Oxford, England, OX1 3PU.

2. Department of Mathematics, University College London, Gower Street, London, England, WC1E 6BT.

3. Department of Applied Mathematics and Theoretical Physics, University of Cambridge, Silver Street, Cambridge, England, CB3 9EW.

where

$$\operatorname{sgn} x = \begin{cases} 1 & x > 0 \\ -1 & x < 0. \end{cases} \tag{1.2}$$

(We shall assume $\eta_0 > 0$ without loss of generality.) For small disturbances, the equations satisfied are the linear shallow water equations

$$u_t - fv = -g\,\eta_x, \tag{1.3}$$

$$v_t + fu = -g\,\eta_y, \tag{1.4}$$

$$\eta_t + (Hu)_x + (Hv)_y = 0, \tag{1.5}$$

where $f$ is the Coriolis parameter, $g$ the acceleration due to (possibly reduced) gravity and $H$ the undisturbed depth of the fluid. For convenience, we take $f > 0$. In the classical case, $H$ is uniform over the whole domain and the result of the adjustment is a jet running along the line of the initial surface discontinuity; i.e., spread about the line $x = 0$. The problem is discussed fully in Chapter 7 of Gill (1982).

To understand the behavior of the atmosphere and ocean, the adjustment of a stratified fluid over bottom topography needs to be considered. Some numerical experiments by Hsieh and Gill (1984) with quite simple configurations indicate that a rich variety of behavior is possible, and these need to be explored in a systematic manner. Here we begin the process by considering a shallow homogeneous layer of fluid with simple step-like topography. A case with undisturbed depth $H$ given by

$$H = \begin{cases} H_- & y < 0 \\ H_+ & y > 0 \end{cases} \tag{1.6}$$

(see Fig. 1) is solved analytically in the next section, and gives rise to some very interesting behavior. Results are illustrated using numerical integrations of the shallow-water equations in a similar geometry. Reduced gravity is used in the numerical experiments, so the deformation scale is the internal Rossby radius. (The shallow-water equations can in this sense be regarded as applying to the bottom layer of a system with a relatively deep overlying layer).

The effect of adding a wall-like coast running perpendicular to the step is investigated next. Numerical experiments are described first, in Section 3, followed by analytic solutions for steady cases in Section 4. The coast acts as a barrier to double Kelvin waves propagating onshore, so behavior for $H_- > H_+$ is very different from that with $H_- < H_+$. With $H_- > H_+$ the double Kelvin waves carry coastal information far offshore: this phenomenon has been associated with flow along the Mendocino escarpment off central California (see Willmott (1984) for a two-layer model). For $H_- < H_+$ however, there is very little disturbance offshore, and longshore currents are concentrated into a narrow boundary layer near the intersection between the step and the coast.

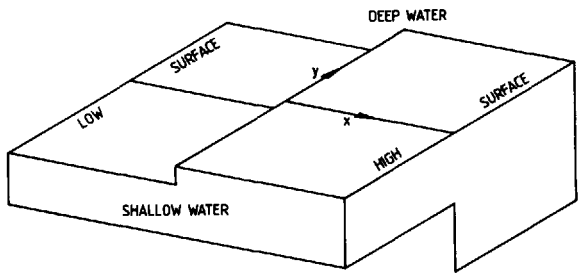


Figure 1. Geometry and initial surface configuration for adjustment over a step. There is a jump in surface displacement along $x = 0$, and in bottom topography along $y = 0$.

In Section 5 we describe some laboratory experiments on geostrophic adjustment of a coastal current in the presence of step topography. A two-layer stratification is established in a rotating channel on both sides of a vertical barrier adjacent to one of the side walls of the channel. Different layer depths are used on the two sides, so that the density interface has an initial discontinuity in depth which is perpendicular to the step change in depth half-way along the channel. This reduced gravity adjustment corresponds closely with the numerical calculations described in Section 4.

It is observed that the coastal current is diverted perpendicular to the coast by the step. If the upper layer is approaching the shallower end, the double Kelvin wave propagates across the tank away from the coast (for $f > 0$), and the current is diverted offshore. On the other hand, when the upper layer is approaching deeper water, the topographic wave travels toward the coast and any transport across the step is confined to a thin boundary layer on the coast. Experiments were also carried out on currents in which there was no upper layer on the outer side of the barrier. In this case, the coastal current is bounded by a front and advection of fluid elements is important. This case, not treated by the theoretical calculations, exhibits the same features as the two-layer case.

## 2. Adjustment over a step

As Rossby showed, the solution of the problem is greatly facilitated by considering the potential vorticity equation. This is derived by first eliminating $\eta$ from (1.3) and (1.4) to get the vorticity equation

$$\zeta_t + f(u_x + v_y) = 0, \tag{2.1}$$

where

$$\zeta = v_x - u_y. \tag{2.2}$$

Then the divergence is eliminated between (2.1) and (1.5) to give

$$\left[\frac{\eta}{H} - \frac{\zeta}{f}\right]_t + \frac{1}{H}[uH_x + vH_y] = 0. \tag{2.3}$$

The step topography has the great convenience that the bottom slope $\nabla H$ is nonzero only along the line $y = 0$ and is zero everywhere else. Thus (2.3) reduces to

$$\left[\frac{\eta}{H} - \frac{\zeta}{f}\right]_t = 0 \text{ except on } y = 0. \tag{2.4}$$

For the initial conditions (1.1), this can be integrated with respect to time to give

$$\frac{\eta}{H} - \frac{\zeta}{f} = \frac{\eta_0}{H} \operatorname{sgn} x \text{ except on } y = 0. \tag{2.5}$$

Furthermore, since for linearized motion, particles move only an infinitesimal distance from their original position, the potential vorticity at any location remains the same for all times.

Consider first the adjustment for large $y$; i.e., far enough from the step for the motion not to be influenced by the step. The flow will take the classical form appropriate to a flat bottom, and in a time of the order of the inertial period will be close to the geostrophic equilibrium for which the velocity $v$ and surface elevations are functions of $x$ only. Thus (1.3) reduces to the geostrophic balance

$$fv = g\eta_x \tag{2.6}$$

and (2.5) becomes

$$\frac{\eta}{H} - \frac{v_x}{f} = \frac{\eta_0}{H} \operatorname{sgn} x. \tag{2.7}$$

These equations are easily solved to give

$$\eta = \eta_0 \operatorname{sgn} x \, (1 - e^{-|x|/a}) \tag{2.8}$$

$$v = (gH)^{1/2} \frac{\eta_0}{H} e^{-|x|/a} \tag{2.9}$$

where

$$a = (gH)^{1/2}/f \tag{2.10}$$

is the Rossby deformation radius. With the sign convention that $\eta_0$ is positive, the velocity $v$ is positive.

We now ask whether the solutions on the two sides of the step are compatible. In particular, is the mass flux of the jet the same on the upstream and downstream sides of the step? The flux can be computed without reference to the detailed solution simply by integrating (2.6) with respect to $x$ to give

$$f \int_{-\infty}^{\infty} v dx = 2g\eta_0. \tag{2.11}$$

The volume flux is thus given by

$$H\int_{-\infty}^{\infty} v\,dx = 2gH\eta_0/f. \tag{2.12}$$

Since $H$ is different on the two sides of the step, the flux is different as well. Suppose $H_- < H_+$. Then the jet approaches the step from the shallow side $y < 0$ with a small flux and leaves the step on the deep side $y > 0$ with a large flux. Clearly something must happen at the step.

In the initial stage of adjustment, the fluid must seek to accommodate the discontinuity in flux at the step by sending out a disturbance from the origin, behind which there will be a flux away from the origin. The only available disturbance with this property would seem to be a double Kelvin wave which propagates along the topographic step with the deep water on its left for $f > 0$ (Longuet-Higgins, 1968). Thus the double Kelvin wave coming from the origin can only affect the region $x > 0$, and it is this property which gives the problem its intriguing asymmetry.

The structure of the double Kelvin wave is very similar to that given by (2.8) and (2.9), but the flow is now directed parallel to the topographic step and the surface elevation approaches $\eta_0$ at both $y = +\infty$ and $y = -\infty$. The surface elevation is continuous across the step, so it must have the form

$$\eta = \eta_0 \operatorname{sgn} x - A(x, t)\, e^{-|y|/a_*} \tag{2.13}$$

where

$$a_\pm = (gH_\pm)^{1/2}/f \tag{2.14}$$

is the Rossby radius determined by the local depth on either side of the step. It follows from the geostrophic relationship (see 1.4)

$$fu = -g\eta_y \tag{2.15}$$

that the along-step velocity is given by

$$u = \begin{cases} \dfrac{gA}{fa_-}\, e^{y/a_-} & y < 0 \\ \dfrac{-gA}{fa_+}\, e^{-y/a_+} & y > 0 \end{cases} \tag{2.16}$$

so the jet is discontinuous over the step. In fact (2.16) shows that the flow has opposite signs on the two sides of the step!

The variable $A$ in (2.13) and (2.16) is a function of $x$ and $t$. The equation it satisfies may be obtained by substituting (2.13) and (2.16) in (1.3) to find $v$, and then applying the condition that the flux $Hv$ is continuous at $y = 0$. Hence $A$ satisfies the

unidirectional wave equation

$$A_t + cA_x = c\,\eta_0\,\delta(x) \tag{2.17}$$

where the wave speed $c$ is given by

$$c = (gH_+)^{1/2} - (gH_-)^{1/2}. \tag{2.18}$$

The solution of (2.17) subject to the condition that $A$ is initially zero is

$$\begin{aligned} A &= \eta_0 \operatorname{sgn} x - \eta_0 \operatorname{sgn}(x - ct) \\ &= \begin{cases} 0 & 0 < ct < x \\ 2\eta_0 & x < ct. \end{cases} \end{aligned} \tag{2.19}$$

The mass fluxes associated with this wave match the fluxes toward and away from the step as follows. First there is a flux away from the origin along the step for $y < 0$. Integrating (2.15) with respect to $y$ gives this flux as

$$H_- \int_{-\infty}^{0} u\,dy = -g\,H_-A/f. \tag{2.20}$$

With $A = 2\eta_0$, as in (2.19) behind the wave front, this matches the flux (2.12) toward the step. Similarly there is a flux toward the origin along the step for $y > 0$, and integrating (2.15) gives the value

$$H_+ \int_{0}^{\infty} u\,dy = -gH_+A/f. \tag{2.21}$$

This matches the flux (2.12) away from the step.

A sketch showing contours of surface elevation for the above solution is given in Figure 2. Details of how the jet turns when it reaches the step have not been calculated analytically, nor have the details at the double Kelvin wave front, so these are shown by broken lines. However, the picture that emerges is most intriguing. Firstly, in the final state, the topographic step acts as a *complete barrier* to the approaching jet, which is completely deflected along the step. The only flow across the step is in the Kelvin wave front, which becomes more and more remote from the path of the original jet as time progresses. The other remarkable property of the solution is the asymmetry. A jet approaching deeper water in the northern hemisphere is deflected to the right. The sign changes with $f$ and a jet approaching shallow water is deflected the other way. Because of these interesting properties, it was decided to carry out laboratory and numerical experiments to further study the problem, and these are reported below.

*Numerical results with no wall.* To illustrate the variety of possible behavior for flow over a step, the linear shallow-water equations (1.3)–(1.5) were integrated numerically in a doubly-periodic domain. Using $gH_{\max} = 9.8$ m$^2$sec$^{-2}$ and taking $f$ at 30N (so the inertial period is one day), the Rossby radius $a$ based on $H_{\max}$ is about 43 K m. For

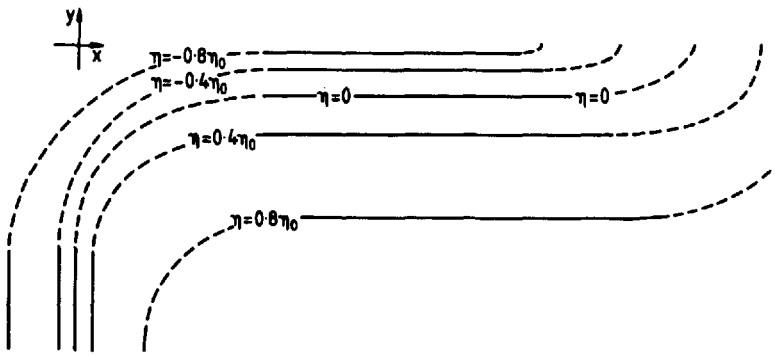


Figure 2. A sketch of contours of surface displacement in the region $y < 0$ after release of the initial configuration in Figure 1. A double Kelvin wave is travelling in the $+x$ direction: details of the flow in the vicinity of dashed contours have not been calculated.

convenience $a$ is used as a length scale, and we define new coordinates

$$(X, Y) = (x, y)/a$$

The topography has

$$H = \begin{cases} \frac{1}{2}H_{\max} & 0 < Y < 20, \quad 60 < Y < 80 \\ H_{\max} & 20 < Y < 60 \end{cases} \tag{2.22}$$

with period 80 in the $Y$ direction (see Fig. 3). The spacing of grid points is $a/2$ in each direction.

A surface displacement is generated by adding the term $F(x)\,T(t)$ to the right-hand side of (1.5), with

$$F(x) = \begin{cases} -\eta_0 & 0 < x < 20, \quad 60 < x < 80 \\ \eta_0 & 20 < x < 60, \end{cases} \tag{2.23a}$$

$$T(t) = \begin{cases} 1 - \cos(2\pi t/\tau) & 0 < t < \tau \\ 0 & \tau < t, \end{cases} \tag{2.23b}$$

where $\tau$ is two inertial periods. The effect is similar to using an initial displacement with the pattern $F(x)$, but substantial gravity and inertial wave 'noise' is avoided by this means.

Figure 4a shows contours of $\eta$ when the forcing term is switched off. Geostrophic adjustment has led to a jet in the $+Y$ direction along $X = 30$, and another in the $-Y$ direction along $X = 10$. The cross-section along $Y = 40$ shows $\eta$ effectively unaffected by the steps. Details of part of the velocity field appear in Figure 4b. Double Kelvin waves can be seen starting to propagate along the steps, in the $+X$ direction at $Y = 20$, and the $-X$ direction at $Y = 60$. Note that the wave direction depends on the nature of

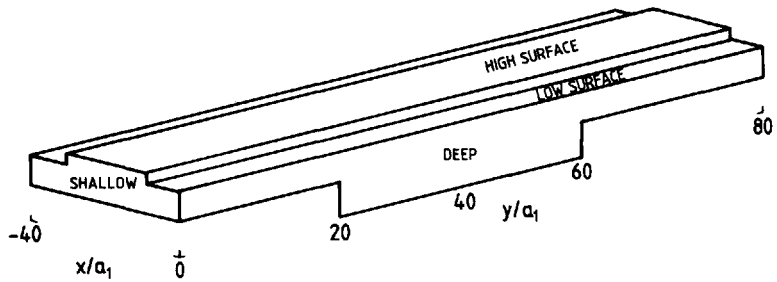


Figure 3. Geometry and effective initial surface configuration for the doubly-periodic numerical experiment. The length unit is the Rossby radius $a$ for the deep region.

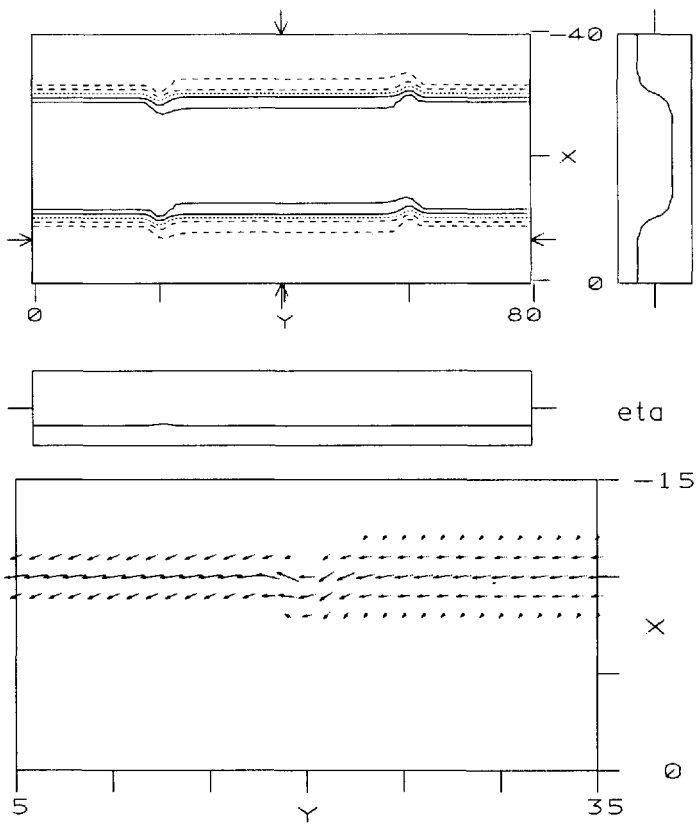


Figure 4. The flow corresponding to Figure 3 after two inertial periods. (a) Surface contours of surface displacement $\eta$ (negative dashed, zero dotted). Cross sections along the arrowed positions appear to the left and below the contour map. (b) Details of the horizontal velocity field near the step along $x/a = 20$ where a double Kelvin wave is beginning to propagate in the $+x$ direction.

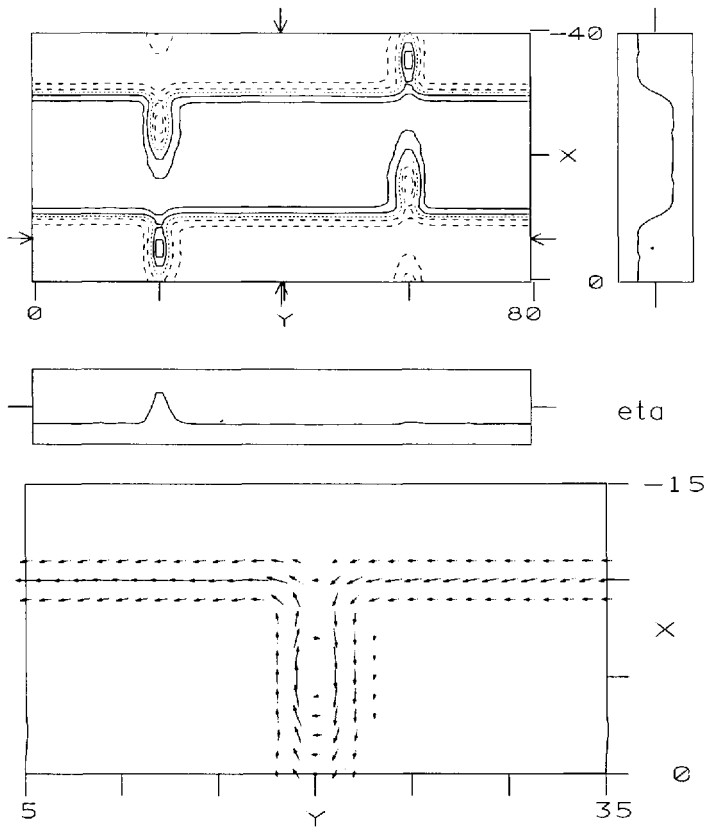


Figure 5. As for Figure 4, but after ten inertial periods (a) surface displacement $\eta$; (b) details of velocity field.

the step and propagates with the shallow water on the right, and not on the direction of the jet.

After 10 inertial periods the waves have travelled about a quarter of the way across the region, as can be seen in Figure 5. Flow far from the steps is virtually unchanged, but currents are diverted along the steps themselves, with very little transport across the steps, consistent with the linearized analysis given above.

## 3. Numerical results with coast

The preceding results are considerably altered when vertical walls running perpendicular to the steps are added. In this section, time-dependent numerical experiments in a periodic channel are described. The topography is almost identical to (2.22), except that the deep ($H = H_{max}$) region is enlarged to $10 < Y < 60$ to defer interaction of one step with another via coastal Kelvin waves, which travel faster in deeper water. Vertical walls are placed at $X = 0$ and $X = -5$. Grid spacing is $a/2$ alongshore and $a/4$

offshore. The height field along $X = 0$ is forced for one 'day' to generate a perturbation: in the absence of the steps this would simply lead to a longshore current near that coast.

The situation after two inertial periods is shown in Figure 6. Contours of $\eta$ reveal double Kelvin waves beginning to travel along the steps. (A small amount of gravity wave 'noise' is also apparent, particularly near $X = -5$, as a consequence of the rather rapid generation.) The cross-section along $Y = 40$, shown to the left of the contour map, effectively shows $\eta$ as unaffected by the steps. The velocity fields in Figures 6b, c show the longshore current being deviated toward the coast near $(X, Y) = (0, 10)$ and away from the coast near (0, 60).

After six inertial periods the double Kelvin waves are well established. The wave travelling away from $X = 0$ along the step at $Y = 60$ has reached the opposite wall: behind it the longshore current has been diverted offshore, with very little flow across the step. Velocity details can be seen in Figure 7c. The pattern here is similar to that seen in the absence of a wall, in the previous section.

The wave travelling toward $X = 0$ along the step at $Y = 10$ is blocked by the coast. The longshore current there is being pinched into a strong, narrow jet next to the coast, as is evident in the velocity field in Figure 7b. Strong cyclonic vorticity is generated as the current crosses the step into deeper water; sufficient to create a return flow offshore. Details here are limited by the resolution of the finite-difference grid, but the flow is confined to the immediate vicinity of the coast. There is very little disturbance offshore, in contrast to the behavior at $Y = 60$, where the flow is diverted away from the coast.

After ten inertial periods coastal waves have travelled from one step to the next, and the flows near each step subsequently influence each other. The double Kelvin wave impinging on the wall at $X = -5$ has generated another coastal wave along that wall, travelling in the $-Y$ direction, as is clear in the contour map in Figure 8a. The velocity structure near $X = 0$, $Y = 10$, shown in Figure 8b, seems to be spreading offshore with a complicated pattern of flow reversals; by far the strongest current is still next to the wall however.

## 4. Steady analytic results with wall

In this section analytic solutions of the linear shallow-water equations are described, for steps supporting double Kelvin waves travelling both toward and away from a vertical coast at $x = 0$ bounding the semi-infinite region $x \leq 0$.

For steady flow, (1.3) to (1.5) reduce to

$$fv = g\eta_x \tag{4.1a}$$

$$fu = -g\eta_y \tag{4.1b}$$

$$(Hu)_x + (Hv)_y = 0, \tag{4.2}$$

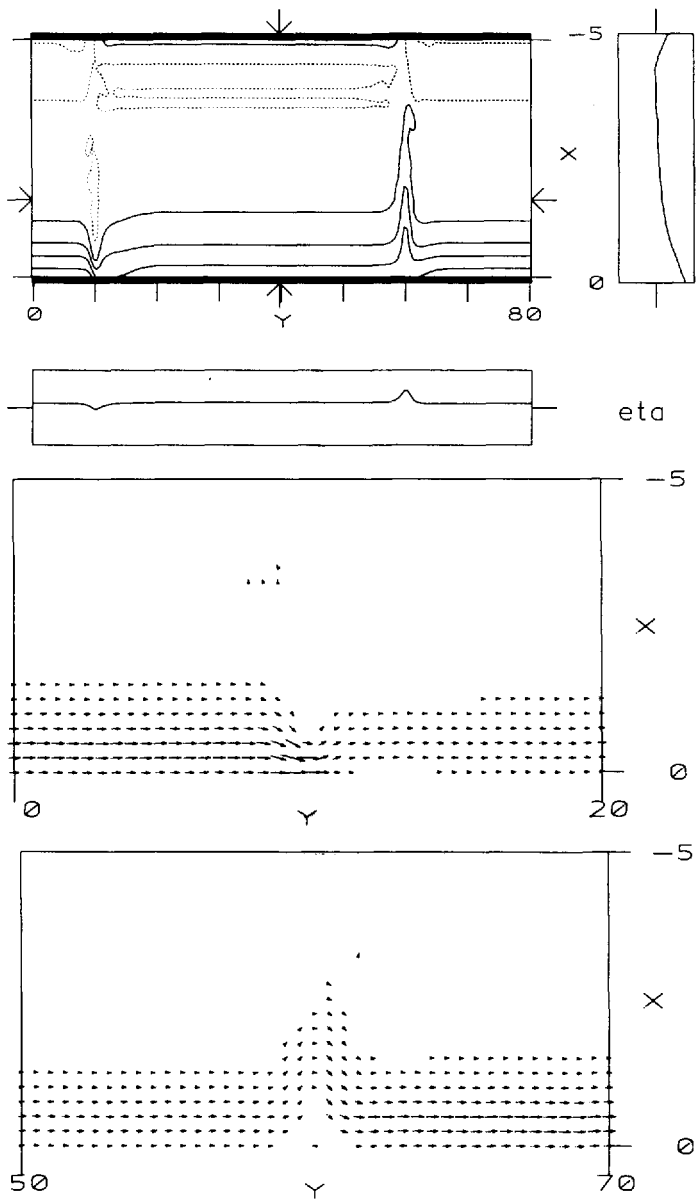


Figure 6. The numerical experiment in a periodic channel, after two inertial periods. There are walls at $x/a = 0$ and $-5$, and steps at $y/a = 10$ and 60, with deep water for $10 < y/a < 60$. (a) surface displacement $\eta$; (b) velocity field near $y/a = 10$, where a double Kelvin wave propagates toward the wall at $x = 0$; (c) velocity field near $y/a = 60$, where a double Kelvin wave propagates away from $x = 0$.

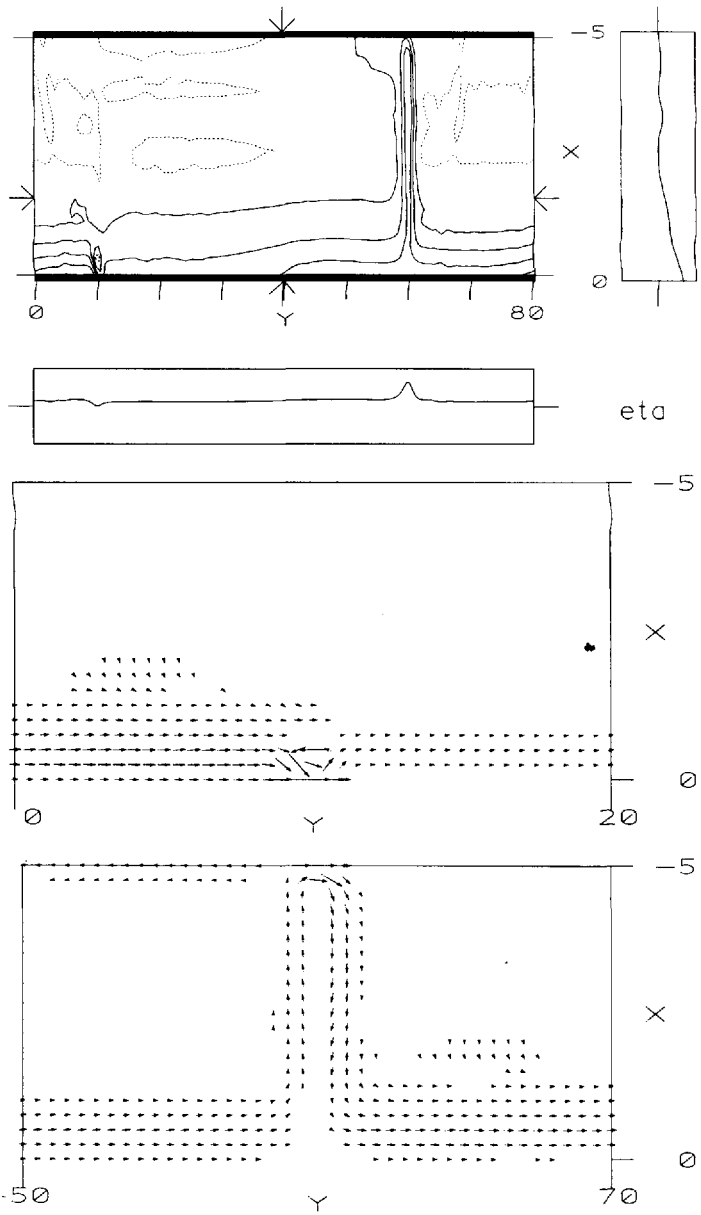


Figure 7. As for Figure 6, but after six inertial periods. (a) surface displacement; (b) velocity field near $y/a = 10$, where there is strong longshore flow at the step/wall intersection; (c) velocity field near $y/a = 60$.

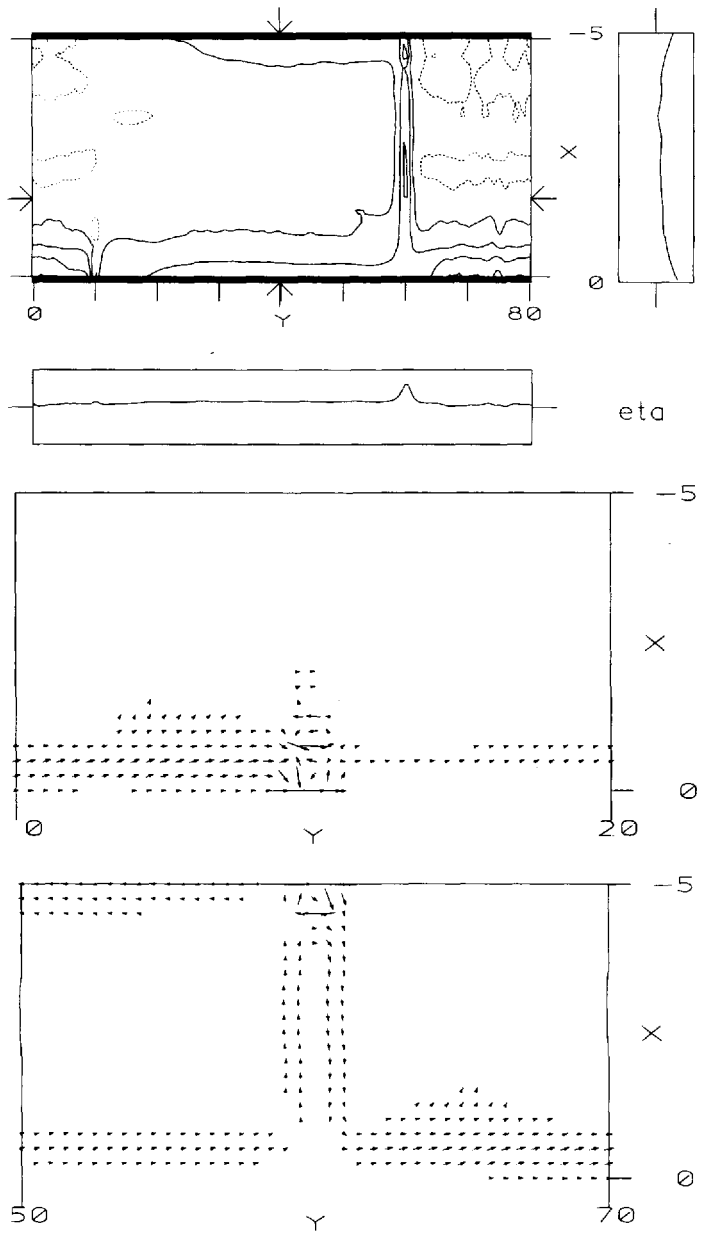


Figure 8. As for Figure 6, but after ten inertial periods. (a) surface displacement; (b) velocity field near $y/a = 10$; (c) velocity field near $y/a = 60$.

and from (2.4)

$$\frac{\eta}{H} - \frac{\zeta}{f} = \text{initial value.} \tag{4.3}$$

For simplicity, we consider an initial surface displacement which is constant to a distance $d$ offshore, and zero thereafter:

$$\eta = \begin{cases} \eta_0 & -d < x < 0 \\ 0 & x < -d. \end{cases} \tag{4.4}$$

As in Section 1, a step runs along $y = 0$, with $H = H_-$ for $y < 0$ and $H = H_+$ for $y > 0$.

From (4.1)–(4.4),

$$a_\pm^2 \nabla^2 \eta - \eta = \begin{cases} -\eta_0 & -d < x < 0 \\ 0 & x < -d. \end{cases} \tag{4.5}$$

We choose $a_-$ as a length scale, and define $(X, Y) = (x, y)/a_-$ and $D = d/a_-$.

*a. No step.* For later reference, we first consider the case $H_- = H_+$, for which there is no longshore dependence. Mass conservation requires

$$\int_{-\infty}^{0} \eta dX = \eta_0 D. \tag{4.6}$$

Using this condition, with continuity of $\eta$ and $\eta_X$ at $X = -D$ and $\eta \to 0$ as $X \to -\infty$, we obtain

$$\bar{\eta}(X) = \eta_0 \sinh D\, e^X + \begin{cases} \eta_0[1 - \cosh(X + D)] & -D < X < 0 \\ 0 & X < -D. \end{cases} \tag{4.7}$$

(An overbar distinguishes the no-step solution.)

At the coast,

$$\bar{\eta}(0) = \eta_0(1 - e^{-D}) = \eta_c \text{ (say).} \tag{4.8}$$

Further, $\bar{\eta}_X = 0$ at $X = 0$, so

$$\bar{v}(0) = 0 \tag{4.9}$$

at the coast.

*b. Double Kelvin wave propagating offshore $H_- > H_+$.* With $H_- > H_+$, double Kelvin waves propagate offshore. Boundary conditions are needed to solve (4.5): in order to obtain these we first consider the situation as $Y \to -\infty$. Because coastal Kelvin waves transmit information in the $+Y$ direction only (keeping the coast on their right for

$f > 0$), we expect $\eta \to \bar{\eta}$ as $Y \to -\infty$. Then, because $u = 0$ at the coast so $\eta$ is constant along the wall, it follows that

$$\eta(0, Y) = \eta_c \quad Y < 0. \tag{4.10a}$$

From (4.1) and (4.2) and continuity of $\eta$, it can be deduced that both $v$ and $Hv$ are continuous across the step, which can only be true if $v = 0$ at the step. Thus in the steady state there is no flow across the step, as suggested by the time-dependent numerical experiments. Hence $\eta$ is constant along the step, and we have

$$\eta(X, 0) = \eta_c \quad X \leq 0. \tag{4.10b}$$

(The double Kelvin wave carries the information $\eta = \eta_c$ away from the coast to set up this state.) Similarly, we find

$$\eta(0, Y) = \eta_c \quad Y \geq 0. \tag{4.10c}$$

These arguments have been confirmed by closed-form solutions of the initial value problem in the rigid—lid limit (Johnson, 1985) and by numerical evaluations of integral solutions to the free-surface problem (Johnson and Davey, 1986).

To solve (4.5) in the region $Y < 0$, we put

$$\eta = \bar{\eta} + \phi \tag{4.11}$$

Then

$$\phi_{XX} + \phi_{YY} - \phi = 0 \tag{4.12}$$

$$\phi(0, Y) = 0 \quad Y \leq 0. \tag{4.13a}$$

$$\phi(X, 0) = \eta_c - \bar{\eta}(X) \quad X \leq 0. \tag{4.13b}$$

A solution can be readily obtained using Fourier transforms. In convolution form,

$$\phi = \frac{|Y|}{\pi} \int_{-\infty}^{\infty} F(X - \xi) G(\xi, Y) d\xi \tag{4.14}$$

where

$$F(X - \xi) = \begin{cases} \eta_c - \bar{\eta}(X - \xi) & \xi \geq X \\ -\eta_c + \bar{\eta}(\xi - X) & \xi \leq X \end{cases} \tag{4.15a}$$

and

$$G(\xi, Y) = K_1[(Y^2 + \xi^2)^{1/2}]/(Y^2 + \xi^2)^{1/2} \tag{4.15b}$$

where $K_1$ is a modified Bessel function.

Typical shapes of $F$ and $G$ are shown in Figure 9 to illustrate the nature of the convolution. This form is convenient because $G$ decreases very rapidly as $|\xi|$ increases,

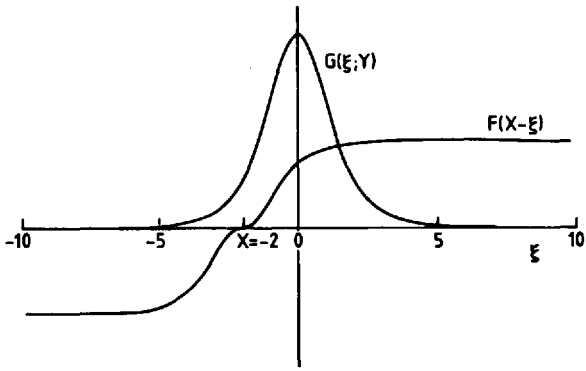


Figure 9. The functions $F$ and $G$ as defined in Eq. (4.15) for the convolution integral, for $X = Y = -2$.

so (4.14) can be rapidly evaluated numerically. (It is sufficient to take $|\xi| < 10$ in the following examples.)

Far offshore, as $X \to -\infty$,

$$\eta \to \frac{|Y|}{\pi} \eta_c \int_{-\infty}^{-\infty} G(\xi, Y)\, d\xi = \eta_c e^Y \quad (Y < 0) \tag{4.16}$$

in agreement with the double Kelvin wave structure discussed in Section 2.

We also find that there is a weak flow reversal at the coast. Because $\eta_c - \bar{\eta} \geq 0$, it follows that $\phi \geq 0$, with $\phi = 0$ only at the coast. Hence $\phi_X < 0$ at the coast: combining with (4.10), the net effect is $v < 0$ at $X = 0$, for $Y < 0$. (This reversed flow decays to zero as $Y \to -\infty$.)

In the region $Y > 0$, a particular solution satisfying (4.5) and (4.10c) is

$$\hat{\eta}(X) = \eta_0[\cosh(\lambda D) - e^{-D}]e^{\lambda X} + \begin{cases} \eta_0\,[1 - \cosh(\lambda(X + D))] & -D < X < 0 \\ 0 & X < -D \end{cases} \tag{4.17}$$

where

$$\lambda = a_-/a_+ = (H_-/H_+)^{1/2}.$$

The complete solution for $\eta$ can then be obtained in convolution form as for the region $Y < 0$, with $\eta \to \hat{\eta}$ as $Y \to \infty$. Note that $\hat{\eta}_X < 0$ at $X = 0$, so there is a flow reversal at the coast associated with the particular solution. This far-field flow reversal is caused by Kelvin waves carrying information from the step along the wall in the $+Y$ direction.

The surface displacement $\eta$ is shown in Figure 10, for $H_-/H_+ = 2$, and initial perturbation width $D = 1$. The contours of $\eta$ are streamlines, and arrows indicate the direction of flow when $\eta_0 > 0$. (The arrows are reversed if $\eta_0 < 0$.) Weak flow reversal near the coast is evident in the enlargement of the step/coast intersection in Figure

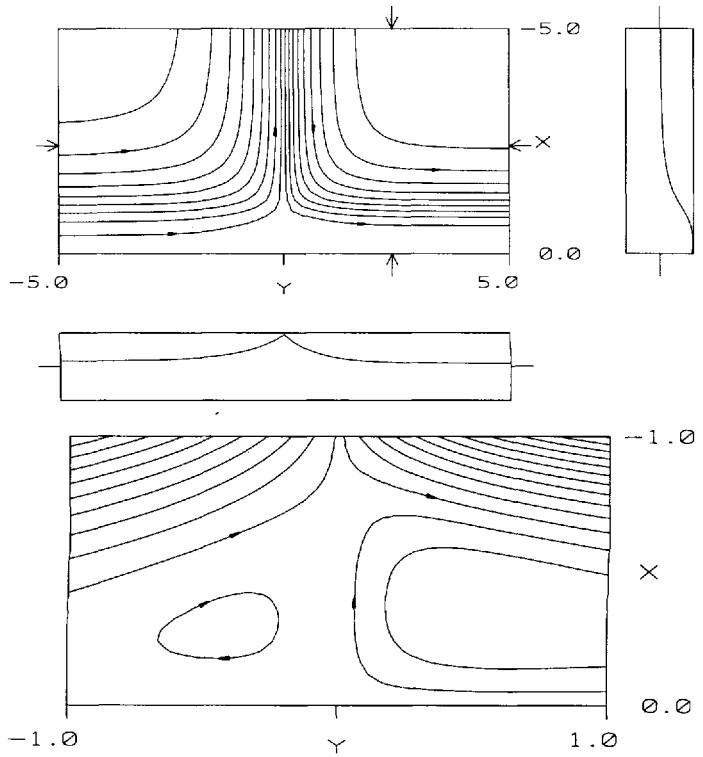


Figure 10. Contours of surface displacement $\eta$ for the steady state with $H_-/H_+ = 2$. (a) large-scale view, (b) enlargement of the step/wall intersection, showing regions of reversed flow; Arrows on contours indicate flow direction for an initially positive disturbance to $\eta$.

10b. In this case the step could be replaced by a wall, and the region $Y < 0$ would be unchanged. Thus this solution is analogous to deflection of a Kelvin wave around a corner (cf Buchwald, 1968).

*c. Double Kelvin wave propagating onshore: $H_- < H_+$.* Again $\eta \to \bar{\eta}$ as $Y \to -\infty$, so the boundary condition (4.10a) still holds. Along $Y = 0$, $\eta$ is constant as before, with no large-scale flow over the step. In this case, however, the constant is determined by double Kelvin waves carrying the information $\eta = 0$ toward the coast from far offshore, and in the steady state

$$\eta(X, 0) = 0 \quad X < 0. \tag{4.18}$$

As noted above, this condition has been confirmed by closed-form solutions in Johnson (1985) and numerical solutions in Johnson and Davey (1986). There is a singularity where the step meets the coast: it arises as a thinning boundary layer in the

time-dependent case. In practice, inertial and viscous (and finite-difference) effects set up a narrow boundary layer.

The constant value of $\eta$ at the coast for $Y > 0$ can be found from mass conservation as follows. The transport across a line between two points $A$ and $B$ (say) in a region of depth $H$ is

$$\frac{gH}{f}(\eta_A - \eta_B) \tag{4.19}$$

Thus there is a transport $gH_-\eta_c/f$ from the region $Y < 0$ across the step via the singular region. This transport is balanced in the region $Y > 0$ if

$$\eta(0, Y) = \frac{H_-}{H_+}\eta_c \quad Y > 0. \tag{4.20}$$

For the region $Y < 0$ we put $\eta = \bar{\eta} + \phi$ as before, and solve (4.12) with

$$\phi(0, Y) = 0$$
$$\phi(X, 0) = -\bar{\eta}$$

to obtain

$$\phi = \frac{|Y|}{\pi}\int_{-\infty}^{\infty} F(X - \xi)G(\xi, Y)d\xi - \frac{2|Y|}{\pi}\eta_c \int_X^0 G(\xi, Y)d\xi. \tag{4.21}$$

The first integral is the well-behaved solution obtained previously; the singular behavior is contained in the second integral. The nature of this term is more apparent for $X^2 + Y^2 \ll 1$, when

$$\frac{-2|Y|}{\pi}\eta_c \int_X^0 G(\xi, Y)d\xi \approx \frac{2}{\pi}\eta_c \arctan(X/|Y|). \tag{4.22}$$

This expression approaches 0 as $X/|Y| \to 0$, and approaches $-\eta_c$ as $|Y|/X \to 0$.

For the region $Y > 0$ we assume that (4.5) still applies. In practice, this equation may not apply everywhere due to the possibly substantial advection of potential vorticity across the step, further modified by boundary layer effects. Our solution using (4.5) should be regarded as a first approximation for a more complicated situation.

The particular solution satisfying (4.5) and (4.20) is

$$\tilde{\eta}(X) = \eta_0[\cosh(\lambda D) - 1 + \lambda^2(1 - e^{-D})]e^{\lambda X} + \\ + \begin{cases} \eta_0[1 - \cosh(\lambda(X + D))] & -D < X < 0 \\ 0 & x < -D. \end{cases} \tag{4.23}$$

A solution in convolution form can then be found as before.

Figure 11 shows $\eta$ for the case $H_-/H_+ = 0.5$, and $D = 1$. The effect of the step is now chiefly confined to the coastal region, in contrast to the outgoing wave case. For $Y < 0$,

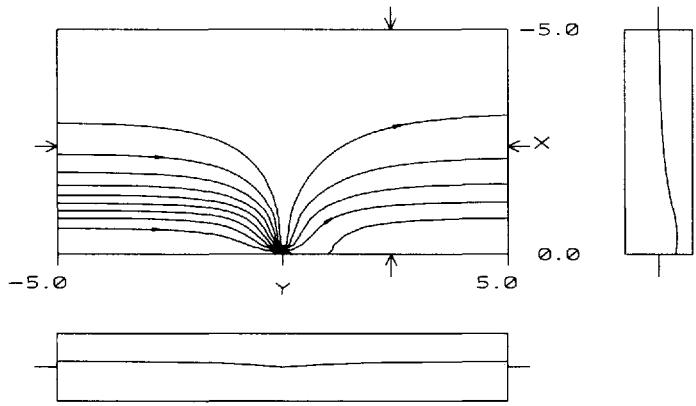


Figure 11. Contours of surface displacement $\eta$ for the steady state with $H_-/H_+ = 0.5$.

there is no flow reversal, and all streamlines pass through (0, 0). In this case flow reversal does appear in part of the region $Y > 0$.

## 5. Laboratory experiments

In this section we report on some laboratory experiments which illustrate the phenomena described in the earlier parts of this paper. These experiments were carried out in a rectangular channel 1.53 m long, 29.4 cm wide and 15.2 cm deep, which was mounted on a direct-drive rotating turntable. The channel was centered on the vertical axis of rotation of the turntable. Inserts constructed from polystyrene blocks were placed on the bottom of the channel to produce a variety of different types of bottom topography. In the experiments described here a rectangular block covering one-half the base of the tank and 5 cm in height was used to produce the step change in depth considered in the theoretical calculations.

Geostrophic adjustment of a two-layer fluid was examined, with the initial discontinuity in the interface height produced by a thin vertical barrier running the length of the tank a distance $L$ from one of the side walls. Salt solution of the required density was first placed in the channel and the system spun up to solid body rotation. A layer of fresh water was then carefully floated on top. The barrier was then placed in position and a further amount of fresh water containing some dye for flow visualization was added in the thin region between the barrier and the tank wall. The whole system was then left to come to solid-body rotation with angular velocity $\Omega = \frac{1}{2}f$, a process which took about an hour. This initial configuration is shown on Figure 12. The experiment was initiated by the vertical removal of the barrier.

The flow was observed by the movement of the dye in the upper layer and from the motion of small paper particles scattered on the free surface. In a few experiments patches of dye were also added to the lower layer in an attempt to infer the flow in that

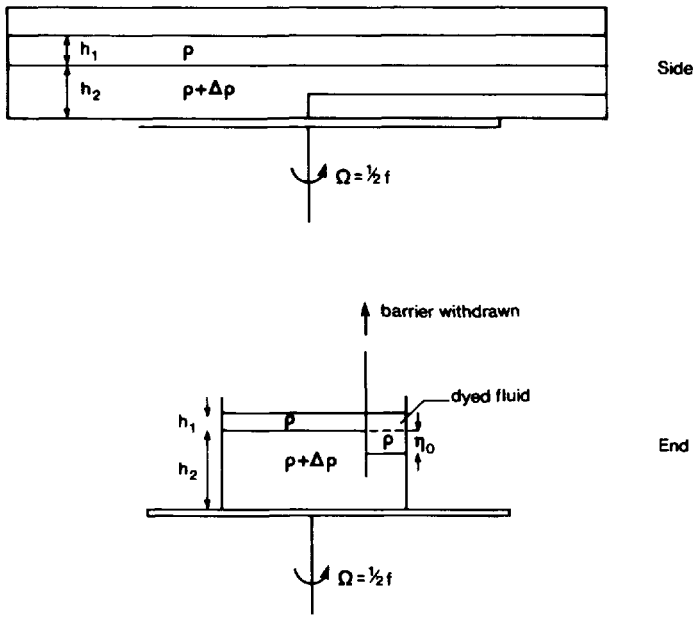


Figure 12. A sketch of the experimental set up. The experiment is initiated by removing the vertical barrier.

layer. Photographs of the flow were taken during the course of the experiment with a camera mounted in the rotating frame.

The depth of the lower layer was in the range 9–14 cm at the deep end and 5–9 cm at the shallow end. The upper layer depth was 1–3 cm and the difference in the upper layer depth on the two sides of the barrier, corresponding to $\eta_0$ of (1.1), varied between 2–4 cm. The values of the reduced gravity $g' = g\Delta\rho/\rho$ between the two layers was varied from 1–21 cm $s^{-2}$ and the Coriolis parameter $f$ took values from 0.5–3 $s^{-1}$. The initial width $L$ of the region between the barrier and the wall varied from 2.5–10 cm. The dimensionless initial width $L/a$, where $a$ is the Rossby radius, took values in the range 0.7–3.1.

A number of experiments were also carried out with a two-layer stratification on the shoreward side of the barrier only (i.e., $h_1 = 0$ on Fig. 12). In this case the geostrophic adjustment in the absence of topography produces a coastal current, the outer edge of which is bounded by a density front at a position approximately $L + a$ from the wall (Griffiths and Linden, 1982). As in the two-layer case adjustment produces a flow parallel to the wall with the upper-layer flow directed so that the wall is on the right when facing downstream for $f > 0$. A flow is also induced in the lower layer but in the opposite sense.

Both the two-layer and frontal currents are unstable to wave-like perturbations which grow along the length of the current. These instabilities grow to large amplitude and form regions of closed streamlines in about 10 rotation periods and appear to gain

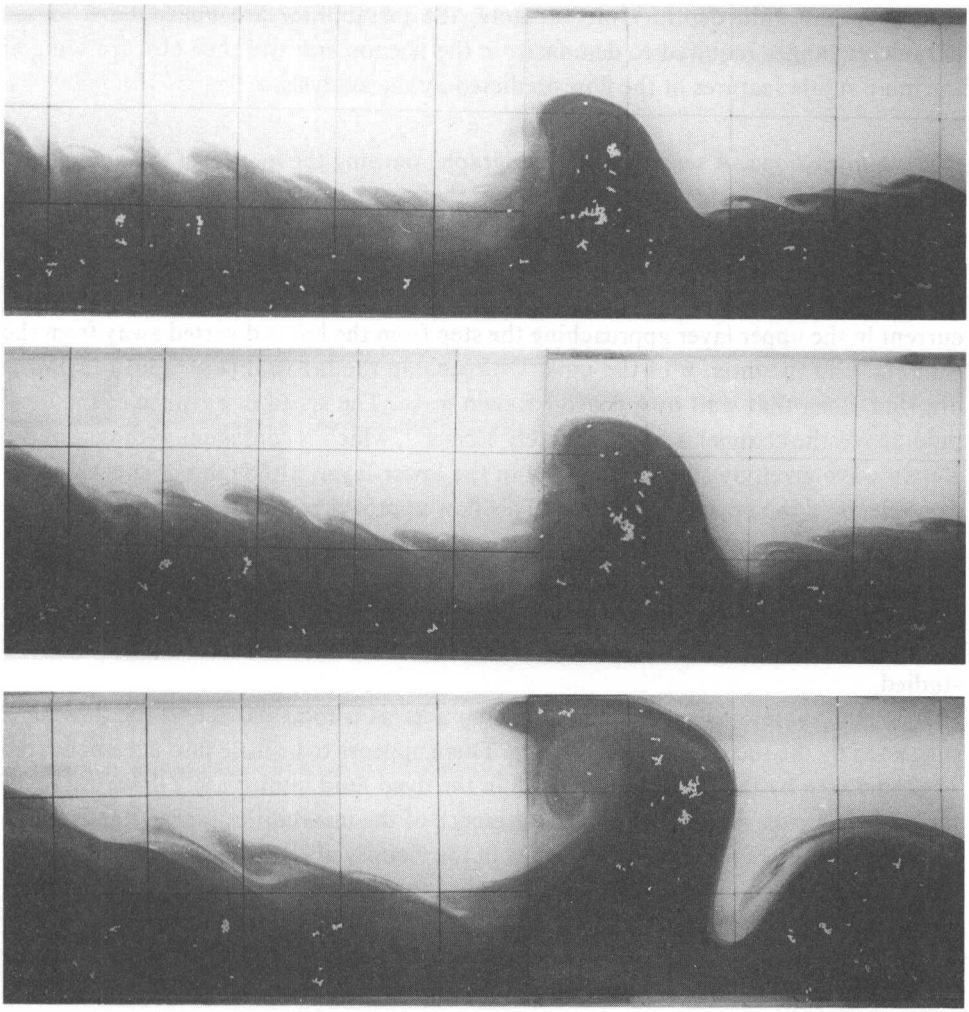

Figure 13. The adjustment of a two-layer flow when the upper layer is approaching the shallow end. The dyed fluid is in the upper layer and was initially confined to the region between the barrier and the wall. The flow across the tank set up by the double Kelvin wave above the step is clearly visible. The plan-view photographs are taken at 2, 3 and 6 rotation periods after the barrier is removed. The flow in the upper layer is from left to right, and the growth of instabilities on the interface can also be seen. In this experiment $L = 8$ cm, $h_1 = 2$ cm, $\eta_0 = 3$ cm, $h_2 = 9$ cm, $g' = 21$ cm s$^{-2}$ and $f = 1.27$ s$^{-1}$. The scale on the floor of the tank is in 10 cm squares.

much of their energy from the sloping density interface remaining after adjustment (Griffiths and Linden, 1982; Killworth, *et al.*, 1984). The initial adjustment and formation of the coastal current occurs within 1 or 2 rotation periods. For the present purposes the presence of the instabilities produces undesirable noise, as we are interested in the mean flow and transport in the current and the response of this to the

change in the fluid depth. Unfortunately, the instabilities are unavoidable in the parameter ranges required to demonstrate the phenomena and they obscure some of the more subtle features of the flow predicted by the analysis.

*a. Two-layer flows.* A sequence of photographs showing the motion of the upper layer in a two-layer flow is shown on Figure 13. In this example the upper-layer flow induced by the adjustment is toward the shallow end of the tank, which is on the right of the picture. The double Kelvin wave, which propagates with the deeper water on the left, travels across the tank above the step in the direction away from the coast. Thus the current in the upper layer approaching the step from the left is diverted away from the wall and into the interior of the tank. On reaching the far wall (Fig. 13c) the flow is diverted along that wall by a coastal Kelvin wave. The speed of advance of the dyed fluid across the channel is approximately 1 cm $s^{-1}$, which is consistent with that of the Kelvin wave given by (2.18). The flow in the lower layer, although not shown in this example, is in the opposite direction. This flow approaches the step from the left (the shallow end) and is diverted out into the interior of the tank by the double Kelvin wave. The width of the diverted flow is observed to be approximately 15 cm, which is about twice the Rossby radius (7.4 cm). This result is consistent with the analytical and numerical calculations, and was found to hold for all the other values of the parameters studied.

It is not possible to say whether the step acts as a total barrier to the flow as is suggested by the theoretical calculations. There appears to be little flow across the step as can be seen by the reduction in width in the dyed fluid immediately downstream of the step visible on Figure 13c, but the presence of the instabilities makes it impossible to determine the exact nature of the flow in the vicinity of the step and the wall.

The case where the flow upper layer is approaching the deep end of the tank is shown on Figure 14. The upper layer is again flowing from left to right, and the double Kelvin wave over the step propagates toward the wall. This case is even more contaminated by the instabilities, since the effect of the Kelvin wave is confined to the region near the wall and the current where the growing waves occur. However, evidence can be seen for an indentation in the dye over the step which increases in size (Figs. 14b and 14c) until it is swamped by the instabilities in the current. The flow across the step is confined to a thin boundary layer near the wall.

*b. Frontal flows.* Similar features were observed in the flow over a step of a coastal current bounded by a front. The two cases are shown in Figure 15. In Figure 15a the upper layer is approaching the shallower end and the double Kelvin wave propagates across the tank away from the wall. The opposite case is shown on Figure 15b where the upper layer is approaching the deep end (the flow of dyed fluid is from right to left and $f < 0$) and the Kelvin wave travels in toward the wall. In this example the reduction in thickness of the current is clearly visible, and the cross-step flow is confined to a thin

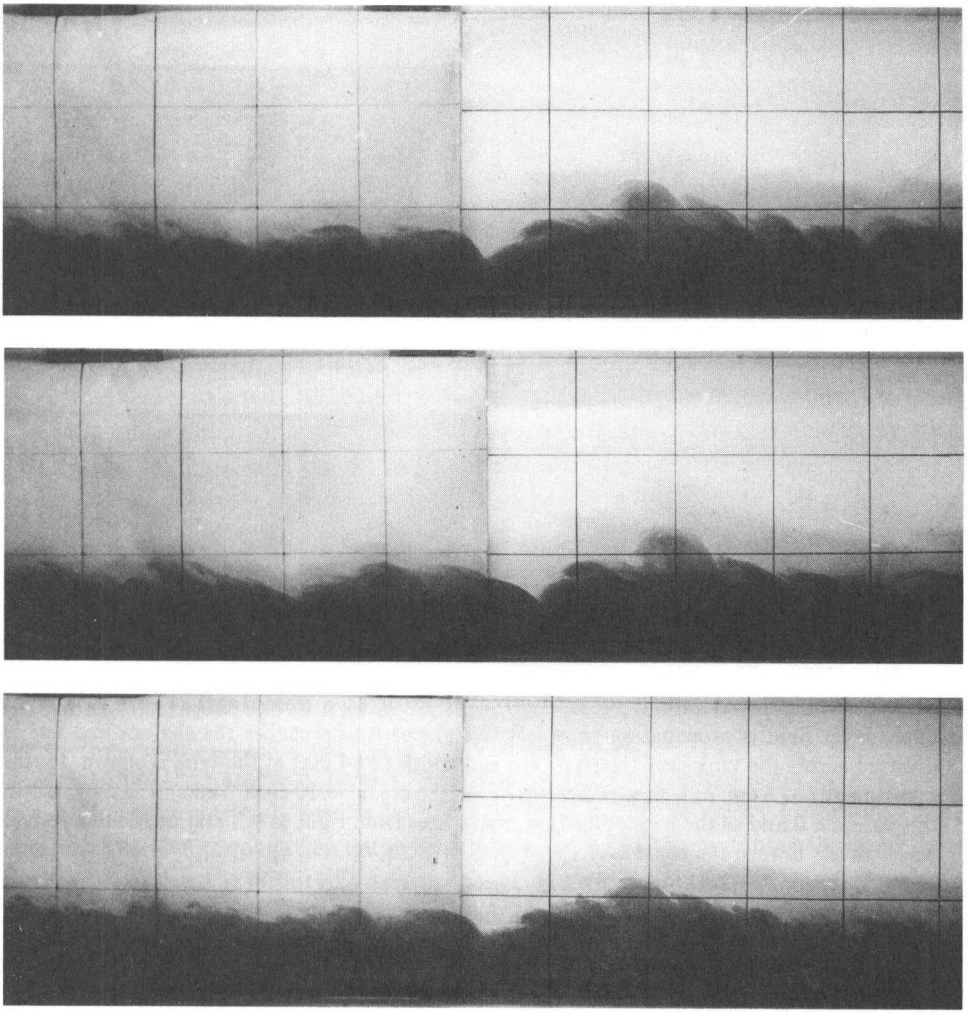

Figure 14. The adjustment of a two-layer flow when the upper layer is approaching the deep end. In this case the double Kelvin wave propagates in toward the wall and the thinning of the current in the vicinity of the step can be seen. The photographs are taken at 2, 3 and 4 rotation periods after the removal of the barrier. The parameters are $L = 5$ cm, $h_1 = 2$ cm, $\eta_0 = 2$ cm, $h_2 = 9$ cm, $g' = 21$ cm s$^{-1}$ and $f = 1.20$ s$^{-1}$.

region near the wall. Again the presence of instabilities makes it impossible to detect features such as the weak recirculating region near the step, predicted by the theoretical calculations (see Fig. 10).

The similarities between the frontal flows and the two-layer adjustment suggests that the basic aspects of the flow in the presence of topography are robust. In the frontal case the diversion of the flow into the interior of the fluid by the step can only be

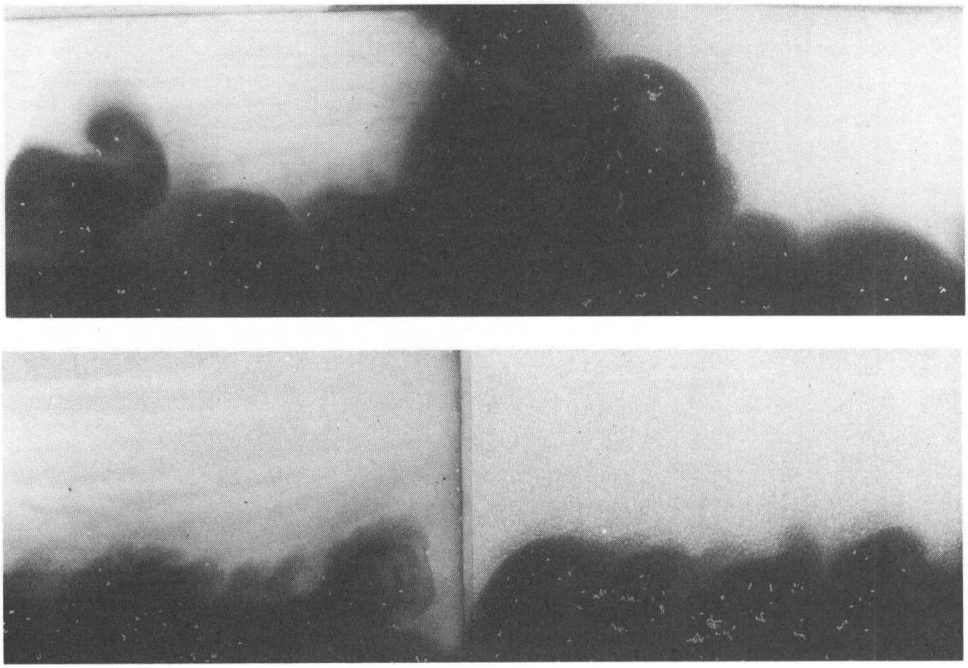

Figure 15. The adjustment of a coastal current bounded by a front. (a) The current of dyed upper-layer fluid is propagating from left to right as it approaches the shallow end and is diverted across the tank over the step. The full width (29.4 cm) of the tank is shown. In this experiment $L = 5$ cm, $h_1 = 0$, $\eta_0 = 2.5$ cm, $h_2 = 10.5$ cm, $g' = 10$ cm s$^{-2}$ and $f = 2.5$ s$^{-1}$. (b) In this case $f < 0$ and so the coastal current propagates from right to left and the double Kelvin wave travels toward the coast over the step. $L = 5$ cm, $h_1 = 0$, $\eta_0 = 2.5$, $h_2 = 10.5$ cm, $g' = 10$ cm s$^{-1}$ and $f = -2.5$ s$^{-1}$.

achieved by advection of fluid particles, since there is no initial stratification to support an internal double Kelvin wave. The preceding theory, dealing only with small displacement of fluid particles, does not address this case but the similarity between the two types of experiment suggests that it does describe the basic dynamics of these large amplitude motions.

## 6. Summary

The effects of step-like topography on geostrophic adjustment have been examined using laboratory experiments and theory based on the linear shallow-water equations. We find that flow normal to the step is diverted into flow along the step, forming a double Kelvin wave which propagates only in the direction with deeper water to the left. The speed of this wave is the difference between the gravity wave speeds on either side of the step. An important result is that transport across the step effectively only occurs at the propagating wave front. Only material located near the step (along the

step in the linear limit) can cross; otherwise the step acts as a complete barrier to approaching flow.

The direction of propagation of the double Kelvin wave also determines the effect of a vertical wall representing a coast. If the geometry allows offshore propagation, then the wall has very little additional effect: any longshore flow is simply diverted along the step away from the wall. However, if double Kelvin waves travel onshore, then flow along the step is blocked and a thin boundary layer forms, within which an intense jet can transport fluid across the step into a coastal current.

Laboratory experiments were carried out with a step across a rotating channel containing two layers of fluid of different density. An alongshore current was either diverted offshore along the step or 'pinched' into a boundary layer, with speeds and horizontal scales in broad agreement with theory. Instability of the alongshore current obscured many details however, particularly of the quantitative flow across the step. Strictly, the shallow-water theory only applies with a relatively deep upper layer, and a two-layer theory is required, but the laboratory results show that the main phenomena can be qualitatively explained by the simple model described here.

In some experiments fronts intersecting the free surface were used. Again, behavior is qualitatively like the simple model, but in this case material transport is important and a more complete theory must take nonlinear advection effects into account. Further laboratory and numerical work with a variety of slopes, rather than steps (not described here), also shows similar features: generally, a broader slope simply gives lower wave speeds and broader disturbances along the slope.

Apart from the numerical results, details of the time-dependent flows have not been given. However, unsteady results for rigid lid flows in this geometry (Johnson, 1985) show a wavefront propagating in the direction given by (2.18) matching the conditions at the wall to those at infinity. Waves propagating away from the wall accelerate while those propagating toward the wall slow and decrease in wavelength. Inclusion of the effect of a free surface (Johnson and Davey, 1986) in the case with outward propagation places a maximum on the wavefront velocity. Free surface solutions for inward propagation approach the rigid-lid solution once the wavelength becomes small compared to the Rossby radius. A narrow boundary layer forms near the wall-step junction in which viscous or advective effects become important.

## REFERENCES

Buchwald, V. T. 1968. The diffraction of Kelvin waves at a corner. J. Fluid Mech., *31*, 193–205.

Gill, A. E. 1982. Atmosphere-Ocean Dynamics. Academic Press, 666 pp.

Griffiths, R. W. and P. F. Linden. 1982. Laboratory experiments on fronts. Part 1. Density-driven boundary currents. Geophys. Astrophys. Fluid Dynamics, *19*, 159–187.

Hsieh, W. W. and A. E. Gill. 1984. The Rossby adjustment problem in a rotating, stratified channel, with and without topography. J. Phys. Oceanogr., *14*, 424–437.

Johnson, E. R. 1985. Topographic waves and the evolution of coastal currents. J. Fluid Mech., *160*, 499–509.

Johnson, E. R. and M. K. Davey. 1986. Free surface and topographic effects in the evolution of coastal currents. (in preparation).

Killworth, Peter D., Nathan Paldor and Melvin E. Stern. 1984: Wave propagation and growth on a surface front in a two-layer geostrophic current. J. Mar. Res., *42,* 761–785.

Longuet-Higgins, M. S. 1968. On the trapping of waves along a discontinuity of depth in a rotating ocean. J. Fluid Mech., *31,* 417–434.

Rossby, C. G. 1937. On the mutual adjustment of pressure and velocity distributions in certain simple current systems. I. J. Mar. Res., *1,* 15–28.

—— 1937. On the mutual adjustment of pressure and velocity distributions in certain simple current systems. II. J. Mar. Res., *2,* 239–263.

Willmott, A. J. 1984. Forced double Kelvin waves in a stratified ocean. J. Mar. Res., *42,* 319–358.

Received: *11 December, 1985;* revised: *17 June, 1986.*